

Supporting Online Material for Adaptation to Climate Across the *Arabidopsis thaliana* Genome

Angela M. Hancock, Benjamin Brachi, Nathalie Faure, Matthew W. Horton, Lucien B. Jarymowycz, F. Gianluca Sperone, Chris Toomajian, Fabrice Roux, Joy Bergelson*

*To whom correspondence should be addressed. E-mail: jbergels@uchicago.edu

Published 7 October 2011, *Science* **334**, 83 (2011)
DOI: 10.1126/science.1209244

This PDF file includes:

Materials and Methods
Figs. S1 to S11
Tables S1 and S2
References

Other Supporting Online Material for this manuscript includes the following: (available at <http://bergelson.uchicago.edu/regmap-data/climate-genome-scan/>)

Climate data for the 948 accessions used in the analyses, result files for the correlation analyses, and a browser that allows for viewing the results in their genomic context.

MATERIALS AND METHODS

Arabidopsis thaliana accessions and genotype data

We chose a set of accessions collected throughout the native Eurasian range of *A. thaliana* from the complete RegMap Project set (<http://regmap.uchicago.edu>) to be used in this analysis (Figure S5). We excluded accessions that were likely to be contaminants (23), leaving us with a set of 948 accessions.

Climate data

We obtained information about climate for each accession included in the analysis. Data were collected for 40 different climate variables. Details about each dataset are shown in Table S1. In summary, data for 23 bioclimatic variables that summarize information about extremes and variability in temperature and precipitation were obtained from the WorldClim project (2if4). We obtained relative humidity data from the NCEP-NCAR climate reanalysis project (25), and data for growing season lengths was obtained from the FAO GeoNetwork

(<http://www.fao.org/geonetwork/srv/en/main.home>). In addition, we used individual station data to calculate two additional variables related to growing season length: the number of consecutive cold and frost-free days. The lengths of the cold and frost-free periods were calculated using data collected from individual stations. Specifically, the numbers of consecutive days when the temperature was below 4 degrees Celsius (the vernalization temperature for *A. thaliana*) and the consecutive number of days when the temperature was above 0 degrees Celsius were calculated for each of 4189 stations across the Northern hemisphere for each of the years from 2005 to 2009. These years were selected because there were very few missing data points for them compared to the previous years for which data were available. For each station, we calculated an average over the 5-year period, and then we interpolated the results using the kriging function in ArcGIS to arrive at an estimate for each *A. thaliana* accession.

Next, we selected a representative subset of the total variables to include in the climate correlation analyses. The total set of 41 variables (latitude and 40 climate variables) was pruned based on the pairwise Pearson correlations of the variables (Figure S10) so that no two variables had an r^2 greater than 0.8. In cases where variables were strongly correlated with one another, the variable with the most obvious link to the ecology *A. thaliana* was selected. The variables used in the analyses were: aridity, number of consecutive cold days (below 4 degrees C), number of consecutive frost-free days, daylength in the spring, growing season length, maximum temperature in the warmest month, minimum temperature in the coldest month, temperature seasonality, photosynthetically active radiation, precipitation in the wettest month, precipitation in the driest month, precipitation seasonality, and relative humidity in the spring. Figures showing the global distribution of each variable that was used for the climate correlation analyses are available at <http://bergelson.uchicago.edu/regmap-data/climate-genome-scan/>.

Calculating correlations with climate

Across the distribution of a species, genetic variants or phenotypes may be strongly correlated with climate due simply to demographic history. Therefore, we used a

method that allowed us to control for population history when we calculated correlations with climate. A second challenge for this type of analysis is that linear model methods are heavily influenced by outliers, resulting in very strong correlations that are driven by one or a few observations. In fact, initial testing showed that linear model methods tended to often identify variants that were driven mainly or exclusively by climatic outliers.

Previous approaches to genome-wide association mapping using a similar scheme and similar statistical methods have dealt with this problem by removing low frequency variants (minor allele frequency < 10%) from the analysis (e.g., (7)). Here, we elected to include these variants in the analysis, but to use a non-parametric method to assess the strength of correlation between each environmental variable and genetic variant (or phenotype) while controlling for population structure. Specifically, we used a partial Mantel test (26, 27) to calculate the Spearman correlation between a given SNP and environmental variable while controlling for population structure using a kinship matrix based on genome-wide genetic variation data. The dependent variable in the model was either a distance matrix of the phenotypes (for analyses that lead to figs S1-S4) or a distance matrix of an individual genetic variant (for the genome-wide scan to identify variants that were strongly correlated with climate). The predictor variable was the pairwise distance matrix of the climate variable and the covariate was a distance matrix based on the pairwise kinship matrix based on the total set of SNPs. Partial Mantel tests were conducted using the ecodist package (28) in R (29) as the method to assess evidence of a correlation.

Because relationships among accessions in *A. thaliana* appear to follow a strong isolation by distance model rather than a model in which there are many discrete populations, we treated each individual separately in the analysis rather than grouping them into populations. This approach has the added benefit that the numbers of samples from any given region are taken into account in the model. The genetic distance matrix was computed based on the variance/covariance (similarity) matrix from the emma.kinship function in the R package EMMA (10).

In addition to calculating correlations with climate using the partial Mantel test, for comparison we also used a non-parametric Wilcoxon rank sum test to compare the distributions of climate between the two alleles of each SNP. This method does not control for demographic history. It should be noted that use of a kinship matrix to control for population structure results in false negatives when the climate variable itself is correlated with kinship. However, the difference between our enrichment results for the partial Mantel tests compared to the Wilcoxon rank sum tests (Fig. 1 and Fig. S6) indicate that we gain significant power by controlling for similarity among accessions.

Phenotype data used in the climate correlation analysis

Phenotypes used in this analysis were collected as part of a previously published project (7). Phenotypic variation represents genetic variation among accessions since, for each phenotype classification, all accessions were planted together in the same growth chamber or in a common garden and in replicates. We calculated correlations between the 13 climate variables and the 107 phenotypes included in Atwell et al. (7) using a partial Mantel test as described above.

Assessing significance for climate correlations

The classic method for assessing significance for the results of partial Mantel tests is to use permutations of the dependent variable (27). We could not use this approach for two reasons. First, it was computationally not practical to run enough permutations to obtain a p-value with precision necessary to find p-values low enough to equate to the level of genome-wide significance at the 0.05 level using a Bonferroni correction (i.e. 2.3×10^{-7}).

Second, with matrices of only 948x948 cells, we would not have enough information to run such a large number of independent permutations. Instead, we ran 1000 permutations for each SNP and each variable and found a very large excess of low p-values compared to that expected if p-values were uniformly distributed (as expected under the null). For the lowest p-value possible with 1000 permutations (0.001), we found between 33,388 and 78,795 SNPs compared to 214 expected. The abundance of very low p-values from the permutations suggests that including the kinship matrix may not completely control for the effects of population history even when permutations are used to assess significance. This is not unexpected and is analogous to situations observed for related methods that use a kinship matrix to control for population history (30).

Some of the observed excess of low p-values may be due to positive (or negative) selection and linkage disequilibrium (LD) between selected sites and surrounding neutral variation. We asked whether removing linked variation reduces the observed excesses of low p-values. To do this, we used the prune function in PLINK (31) to select representative sets of SNPs based on pairwise r^2 (with a window size of 1000 SNPs). Then, for a range of r^2 cutoffs, we calculated the proportion of SNPs with permutation p-values less than 0.001. These results show that the proportion of low p-values tends to decrease substantially as more SNPs are filtered from the dataset (Fig. S11), revealing an over-representation of SNPs in fairly strong LD among SNPs with permutation p-values less than 0.001. Given that we observed other evidence of sweeps (as described in the main text), this could imply a genetic draft scenario, in which a fairly large number of sweeps have carried linked genetic variation to high frequency (16), or widespread background selection in the genome of *A. thaliana* (15).

Given the uncertainty of the permutation p-values, we used the following alternative methods to ask whether the tail of the distributions of climate correlations were likely to be enriched for true signals of selection.

Comparison of climate correlation signals across annotation categories of variants

To determine whether SNPs likely to be functional were over-represented in the tail of the distribution with climate, we asked whether the proportions of variants in three categories (intergenic, synonymous (S) and nonsynonymous (NS)) relative to the proportions of the same variants overall differed from unity. First, to ask whether these categories were over-represented with the climate variables as a group, we calculated enrichment in the 1% tail of a composite variable, the ranked minimum rank across all climate variables. More specifically, we ranked the results from the individual climate variables to create a statistic that is sometimes referred to as an ‘empirical p-value’. Then, we found the minimum across the set of 13 climate variables and created a new rank statistic based on this vector of minima. This variable allowed us to test climate overall for evidence of enrichment in a single test. To assess significance for observed

enrichments, we conducted 10,000 permutations and compared the observed enrichment to that found in the permuted datasets. For each permutation, a new set of SNPs was chosen by shifting the locations of the SNPs in the functional category under test by a randomly chosen number between 1 and one less than the total number of genotyped SNPs. This scheme results in permutation sets that resemble the original set with respect to linkage disequilibrium. We used the same methodology described above for testing for enrichment for individual climate variables, a minimum rank statistic across variables from the Wilcoxon rank sum test results as well as for the tests of individual variables. Finally, we tested for enrichments in the proportion of NS relative to S SNPs and assessed significance using the permutation methodology described above.

Assessing whether alleles at strongly correlated variants predicts fitness in a particular environment

To ask whether the set of alleles with the strongest climate correlations could predict variation in fitness for a set of accessions planted in the same environment, we used fitness data collected for a set of 179 accessions originating from a wide geographic range but grown together in a common garden in Lille, France. The experimental design and growth conditions of the common garden experiment have been fully described elsewhere and correspond to the 2008-2009 experiment (9). Briefly, the experiment was organized in a three blocks design, each block being an independent randomization of two replicates per natural accession. For plants of two randomly chosen blocks, fitness was approximated by the total silique length (32), which is strongly correlated with seed count (21). The number of accessions used in our analysis after removing 15 likely contaminants (23) and 17 from outside of Eurasia was 147.

First, we selected the set of 254 SNPs that were in the 0.01% tail of the 13 climate correlation distributions. Next, we pruned SNPs based on LD using PLINK ((31)). In this step, we selected SNPs with r^2 less than 50% from each 100 kb region where there was a climate-correlated SNP, and we preferentially chose the SNP with the strongest correlation. Then, we determined which variant was likely to be favorable in Lille by identifying the set of accessions that share a similar climate from the complete set of 948 accessions, i.e., those within 0.1 standard deviations from the Lille climate based on the distribution of climate for all 948 accessions. Next, we asked which allele had a higher frequency in this set relative to the frequencies outside of Lille. Finally, we counted the number of these alleles (i.e., those expected to be favorable in Lille) for each of the 147 accessions and asked whether this count of ‘favorable’ alleles predicted relative fitness (approximated by total silique length) among the accessions. We assessed evidence of correlation between the number of favorable alleles and fitness using the `cor.test()` function in R (29). To assess significance for the correlation coefficient, we compared the result from the actual data to a null distribution of coefficients from 1000 permutation sets. For each permutation, a new set of SNPs was chosen by shifting the positions of the actual climate correlated SNPs by a randomly chosen number between one and one less than the number of genotyped SNPs. For each of these sets of SNPs, we used the same analysis methodology as described above to prune based on linkage disequilibrium to determine which allele should be favorable in Lille.

The permutation scheme should correct for variation in fitness in Lille due to other factors related to geographic or genetic distance from this site so that the p-values

from this analysis should be conservative. However, the correlation coefficient may be overestimated when distance is not included in the model. Therefore, we also conducted the analyses using models that include either genetic and/or geographic distance from Lille (based on all 214,435 SNPs). We modeled the effect of the number of favorable alleles on fitness while controlling for either geographic or genetic distance from Lille. We found that the coefficient drops only slightly to 0.3516 ($p=0.009$) and 0.3442 ($p=0.005$) from 0.4202 ($p=0.008$) when geographic and genetic distance are included as covariates in the model, relative to a linear model with no covariates. Geographic distance was computed simply by calculating the Euclidean distance and genetic distance was approximated by the vector of genetic distances from the accession that was collected at the closest point to Lille from a distance matrix calculated using a kinship matrix produced in the R package EMMA (33).

Clarifying which biological functions were important for adaptation to the environment

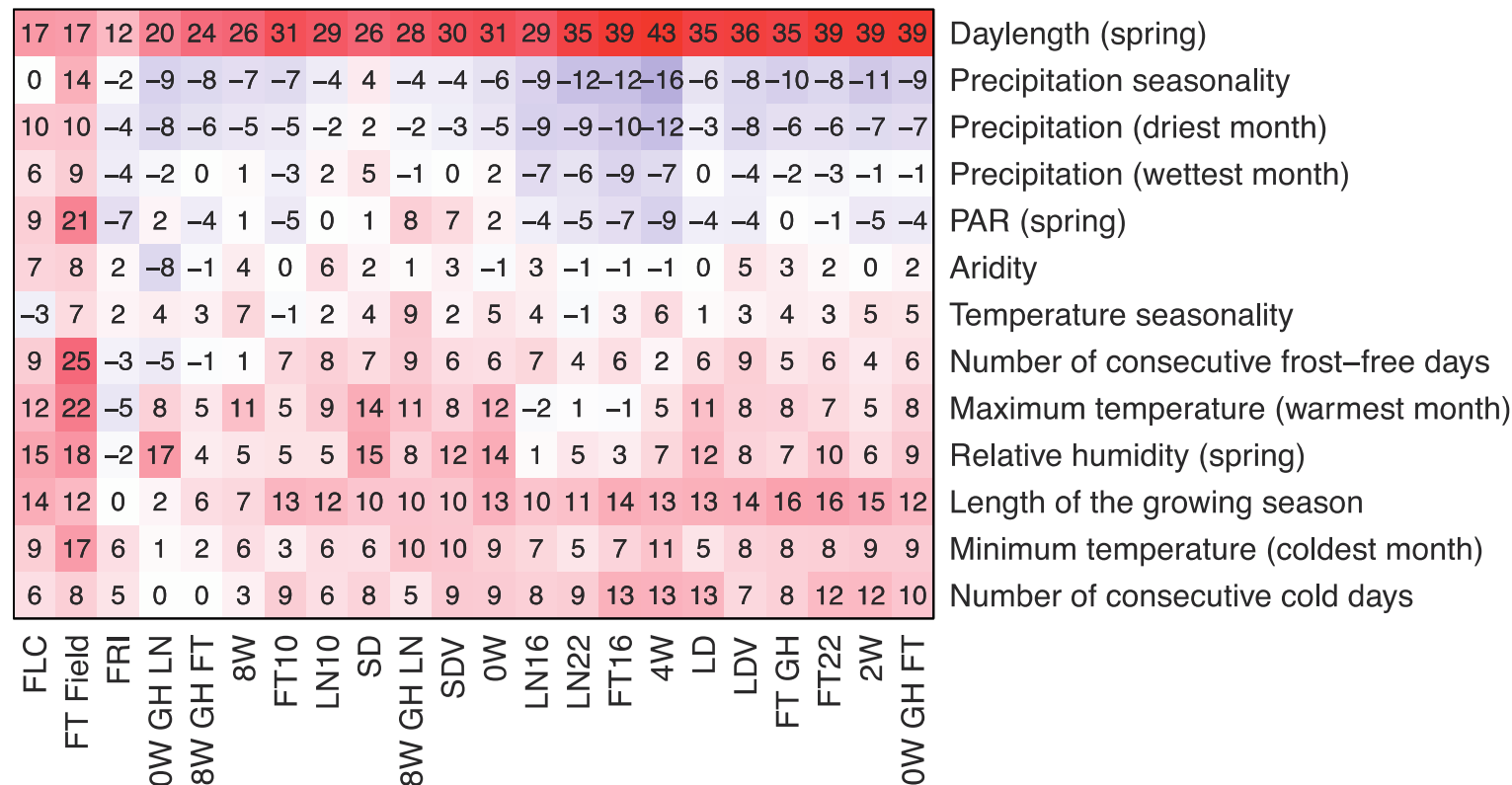
To determine which biological processes were important during adaptation to climate, we tested for an over-representation of SNPs from each of 732 Gene Ontology Biological Processes from the GOslim set (34) (obtained from (ftp://ftp.arabidopsis.org/home/tair/Ontologies/Gene_Ontology/) in the tails of the climate correlation distributions. Specifically, we asked whether each biological process was enriched in the 1% tail of the distribution of correlation coefficients for each climate variable relative to other genic SNPs. 10,000 permutations were run to assess significance using the same methodology described for annotation categories.

Assessing the distributions of geographic extents of SNPs

We calculated the geographic extent of each SNP using by finding its complex hull using the spatial analysis package for ArcGIS 10.1. Then we ranked SNPs based on where they fell in the overall distributions of complex hulls. For plots showing the distribution complex hulls in the 1% tail of the climate correlation distributions we clumped SNPs using the clump function in PLINK to remove redundancy in the data. The parameters used for clumping were the same as in the fitness analysis.

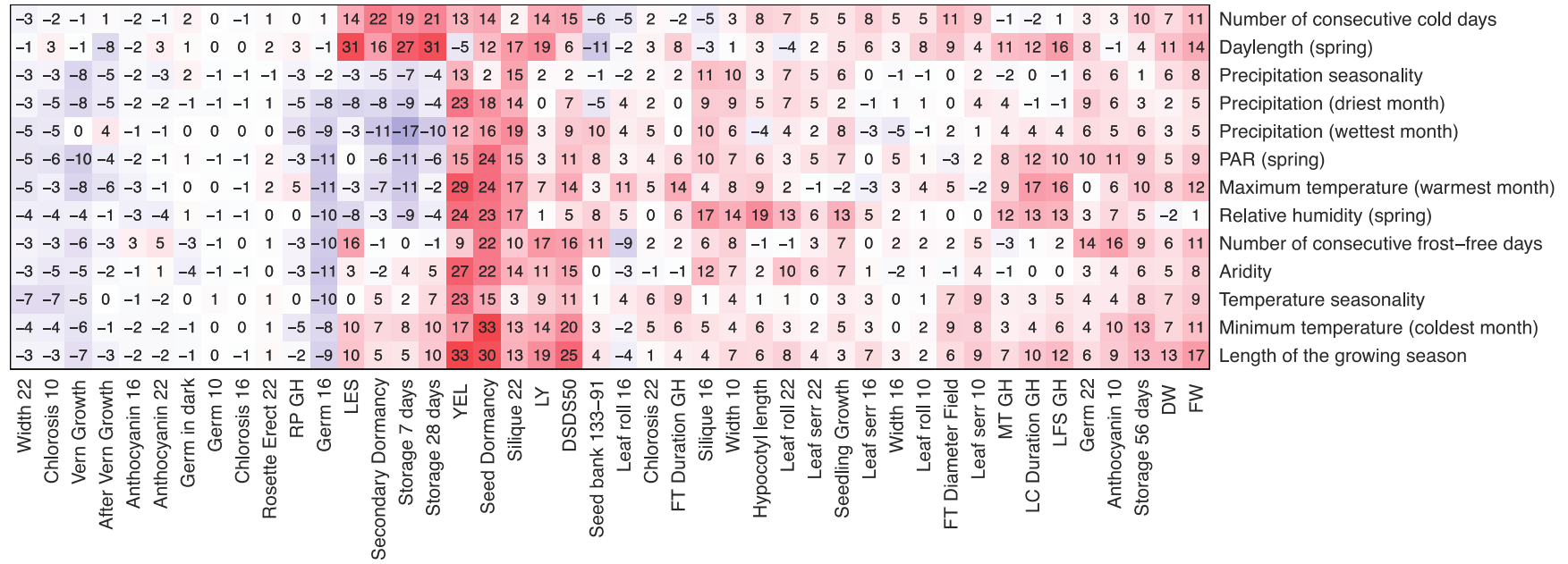
SUPPLEMENTARY FIGURES

Fig. S1.



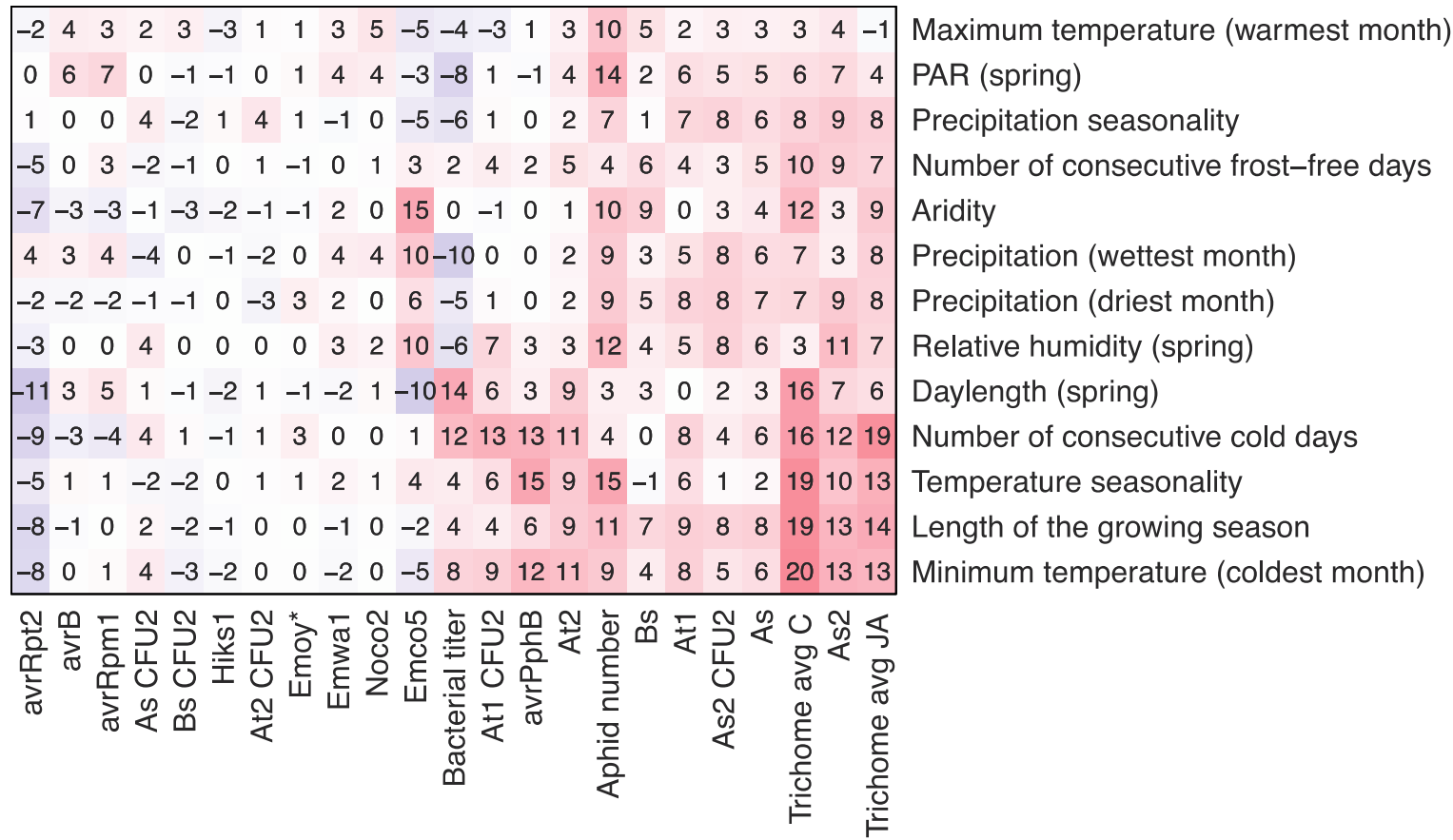
Correlation matrix of partial mantel correlations between climate variables and flowering time phenotypes, where kinship is included as a covariate in this model. Numbers shown in the heatmap are Spearman partial correlation coefficients multiplied by 100. Detailed definitions for each phenotype can be accessed at <https://cynin.gmi.oeaw.ac.at/home/resources/atpolydb>.

Fig. S2



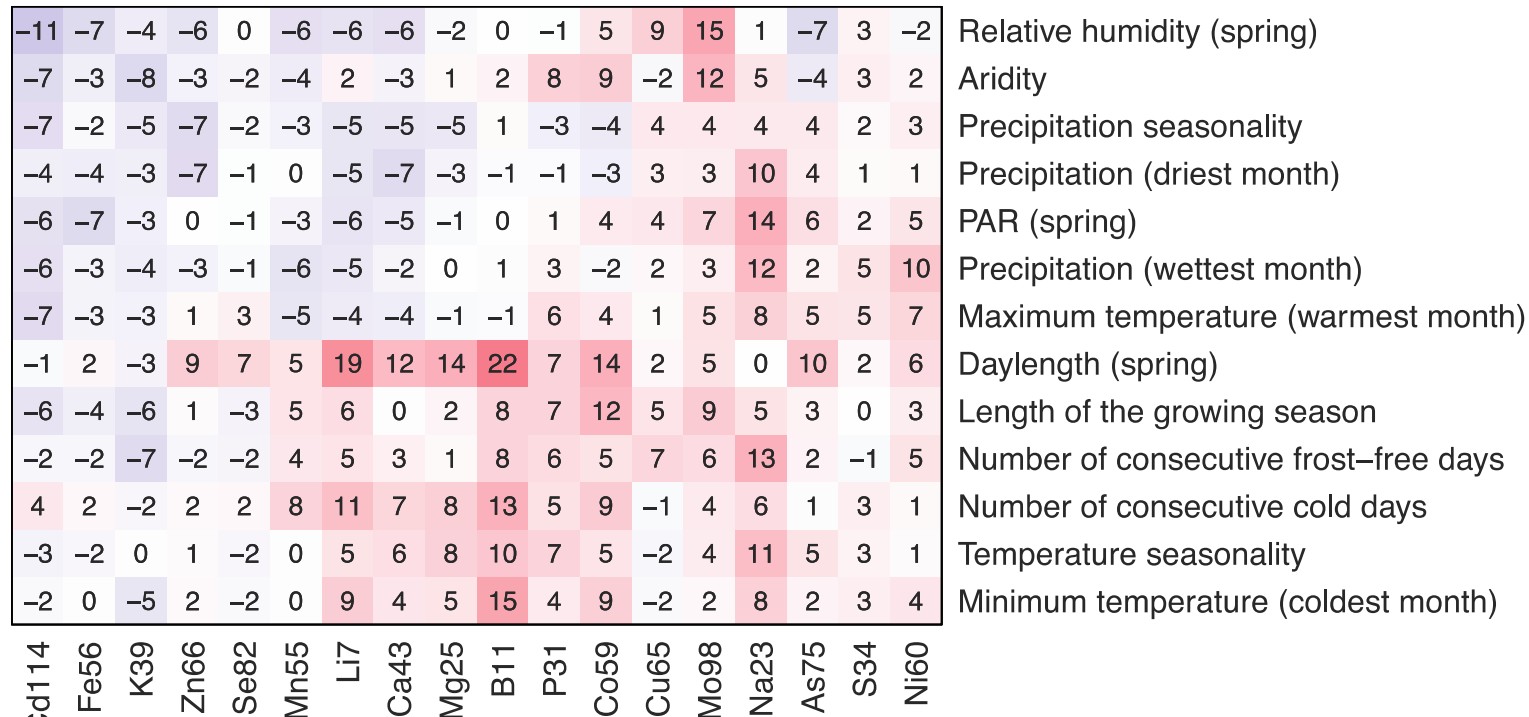
Correlation matrix of partial mantel correlations between climate variables and developmental phenotypes, where kinship is included as a covariate in this model. Numbers shown in the heatmap are Spearman partial correlation coefficients multiplied by 100. Detailed definitions for each phenotype can be accessed at <https://cynin.gmi.oeaw.ac.at/home/resources/atpolydb>.

Fig. S3



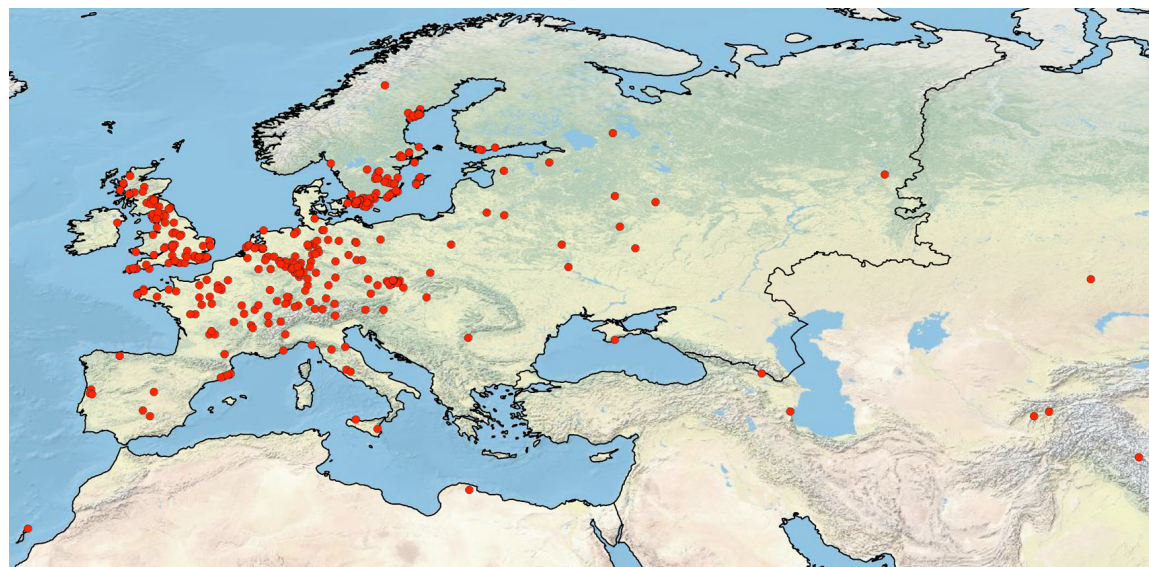
Correlation matrix of partial mantel correlations between climate variables and defense phenotypes, where kinship is included as a covariate in this model. Numbers shown in the heatmap are Spearman partial correlation coefficients multiplied by 100. Detailed definitions for each phenotype can be accessed at <https://cynin.gmi.oeaw.ac.at/home/resources/atpolydb>.

Fig. S4



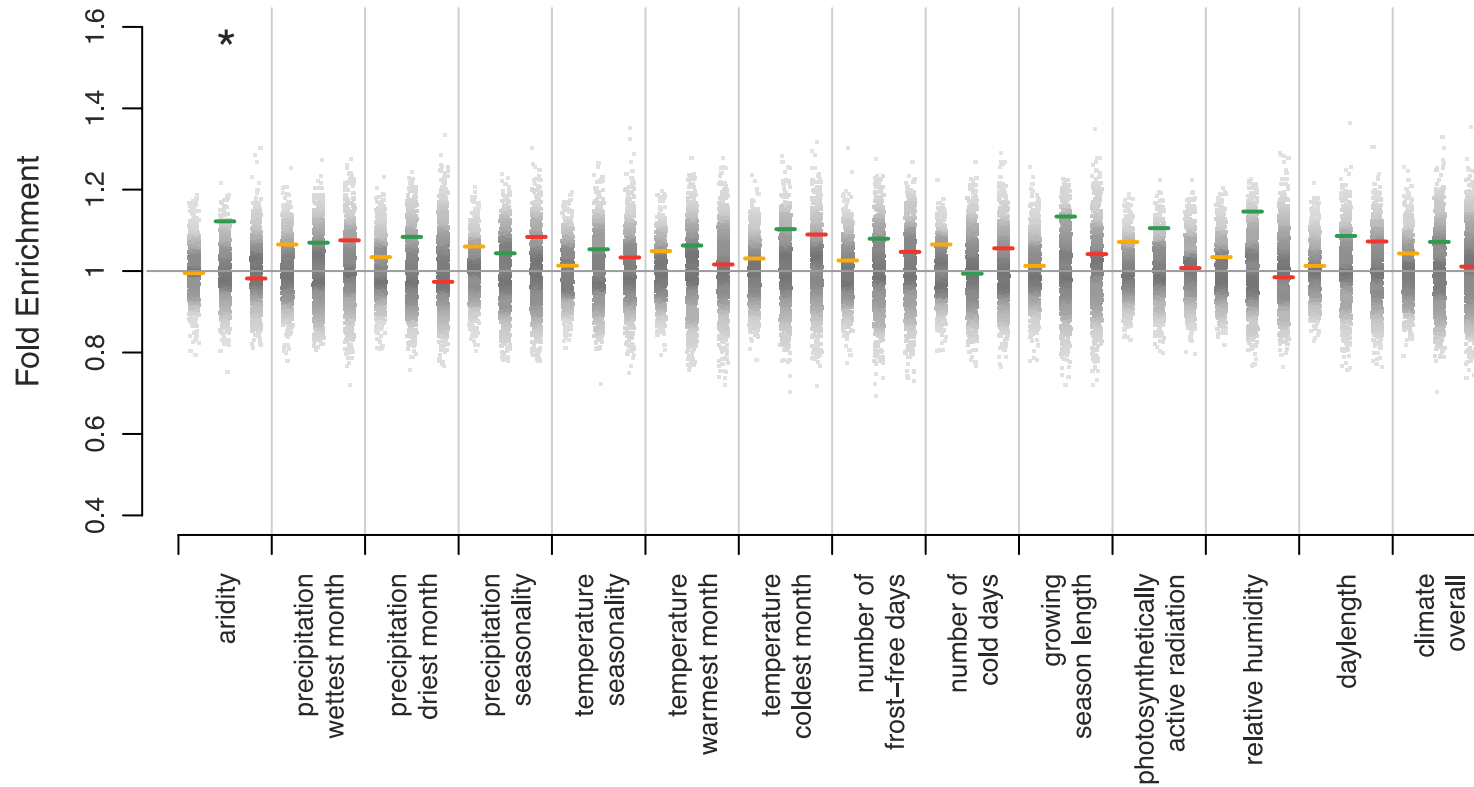
Correlation matrix of partial mantel correlations between climate variables and ionomic phenotypes. Kinship is included as a covariate in this model. Numbers shown in the heatmap are Spearman partial correlation coefficients multiplied by 100. Detailed definitions for each phenotype can be accessed at <https://cynin.gmi.oeaw.ac.at/home/resources/atpolydb>.

Fig. S5



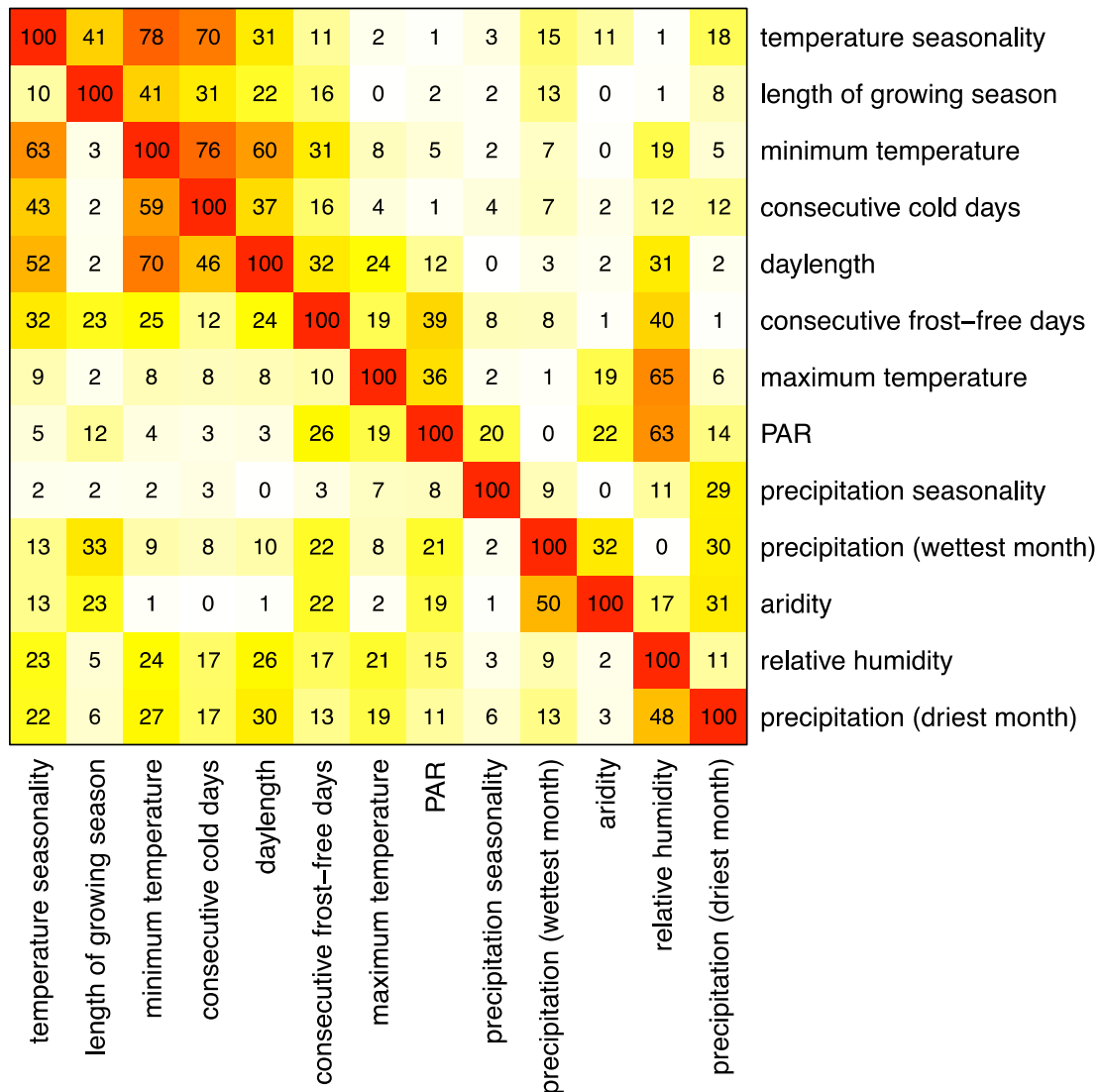
Total set of 948 accessions used in this analysis

Fig. S6



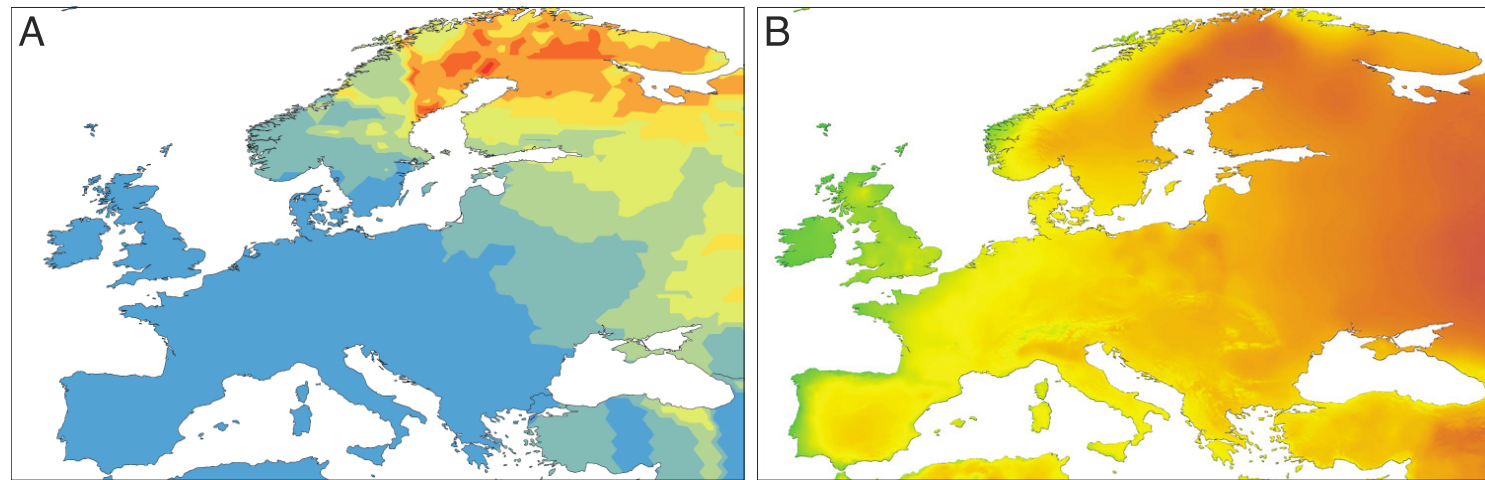
Enrichment of 3 SNP classes with the Wilcoxon signed rank test scan, which does not control for population history. The figure shows enrichment of amino acid changing SNPs (red), synonymous SNPs (green), and intergenic SNPs (yellow) in the 1% tail of the distributions for each individual climate variable as well as for climate overall (using a rank statistic based on the minimum rank across climate variables). Enrichments shown are relative to the proportion of each class of SNPs in the genome overall. Gray dots show the distribution of results of 1000 permutations. The gray line shows the expected enrichment under the null hypothesis of no enrichment. Only one category was significantly enriched ($p < 0.05$); it is denoted by an asterisk.

Fig. S7



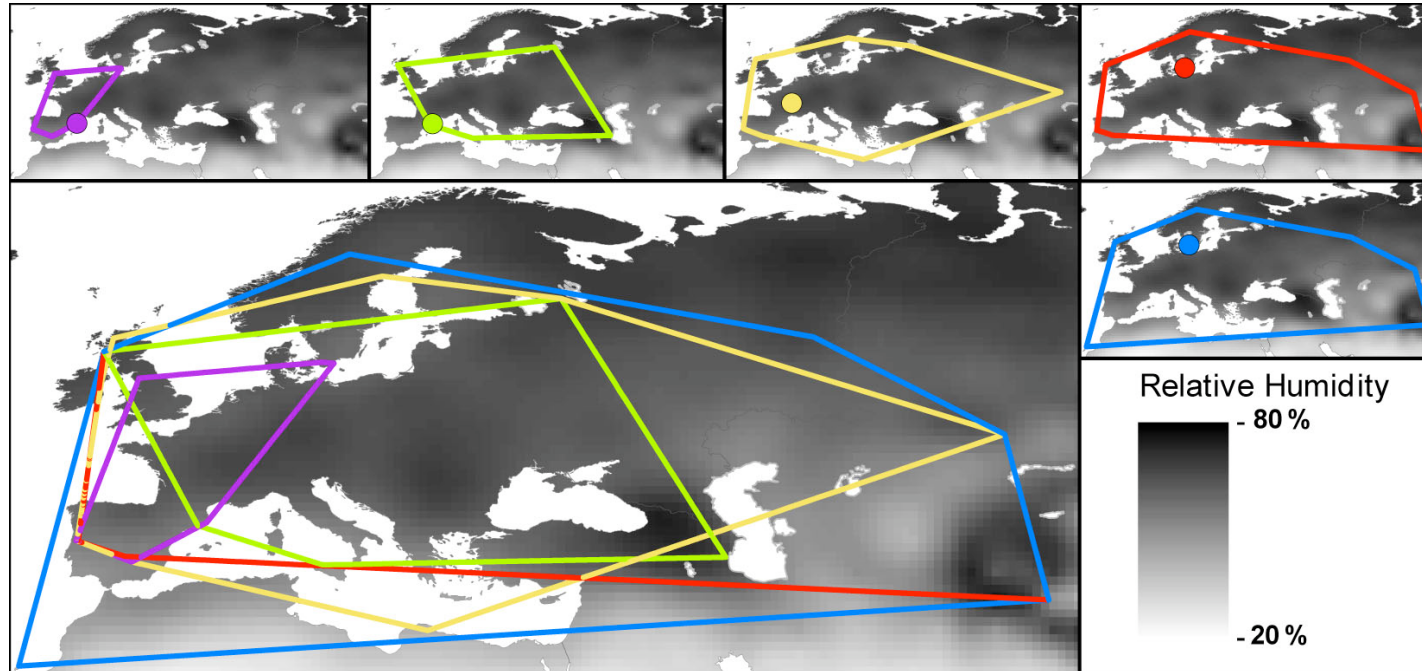
Pairwise matrix of similarity between climate variables. The numbers in the top-right half are the Pearson's r^2 between pairs of variables multiplied by 100. The numbers in the bottom-left are the proportion of SNPs that overlap between the two variables compared.

Fig. S8



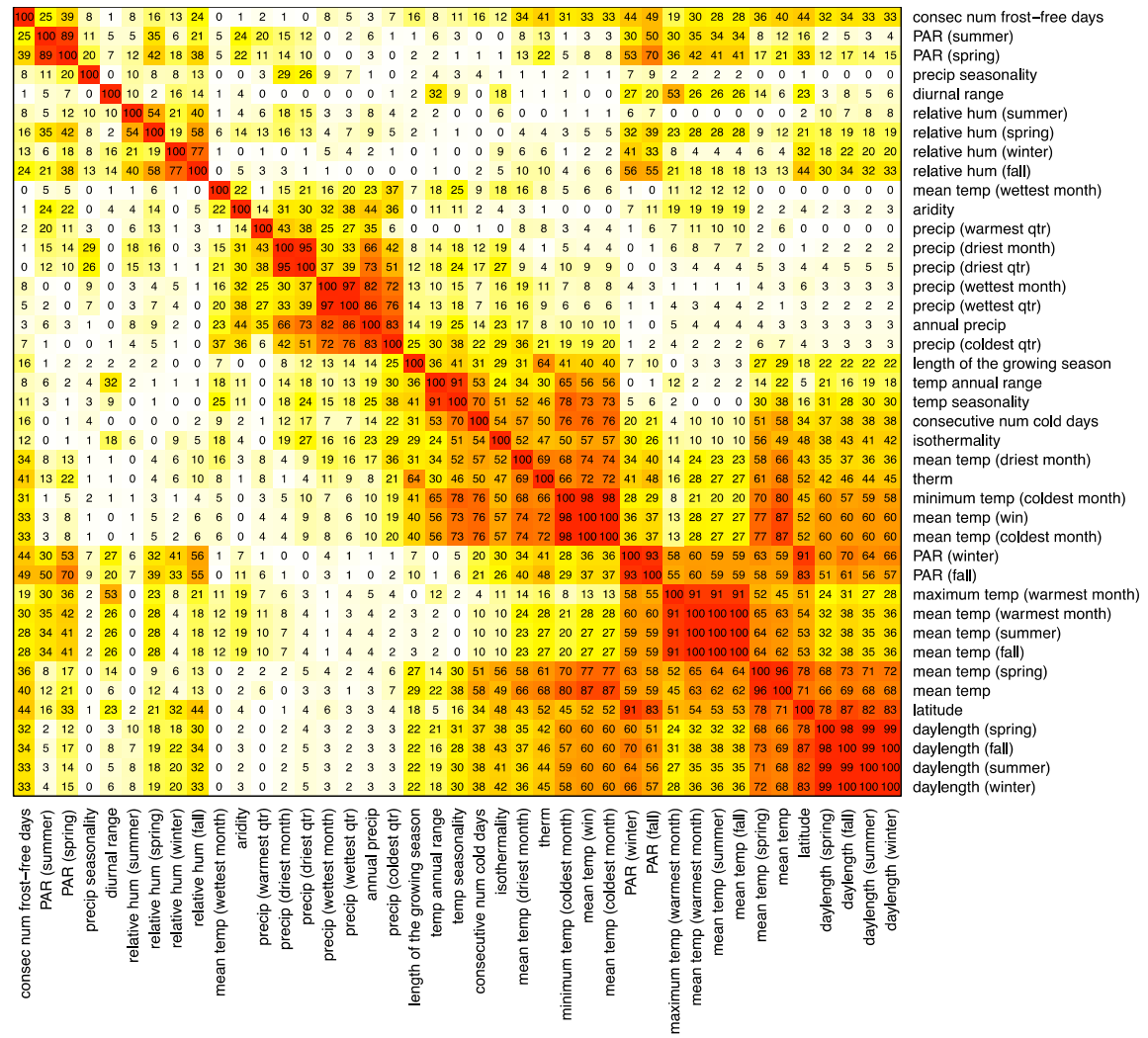
An example of an allele that may have pleiotropic phenotypic effects and thus be correlated with multiple climate variables is tagged by a SNP in *TTG1* (transparent test glabra). This SNP has the strongest correlations in scans with temperature seasonality and minimum temperature and is also strongly correlated with daylength (rank = 50/214435). The gene is involved in purple anthocyanin production, trichome patterning and epidermal cell fate specification (35), three phenotypes that are likely to play roles in both leaf temperature regulation and UV damage. (A) Interpolated distribution of the *TTG1* SNP with the strongest correlation with temperature seasonality and minimum temperature (frequencies range from 0 (blue) to 0.8 (red)). (B) Distribution of temperature seasonality (values range from 27 (green) to 112 standard deviations (orange)).

Fig. S9



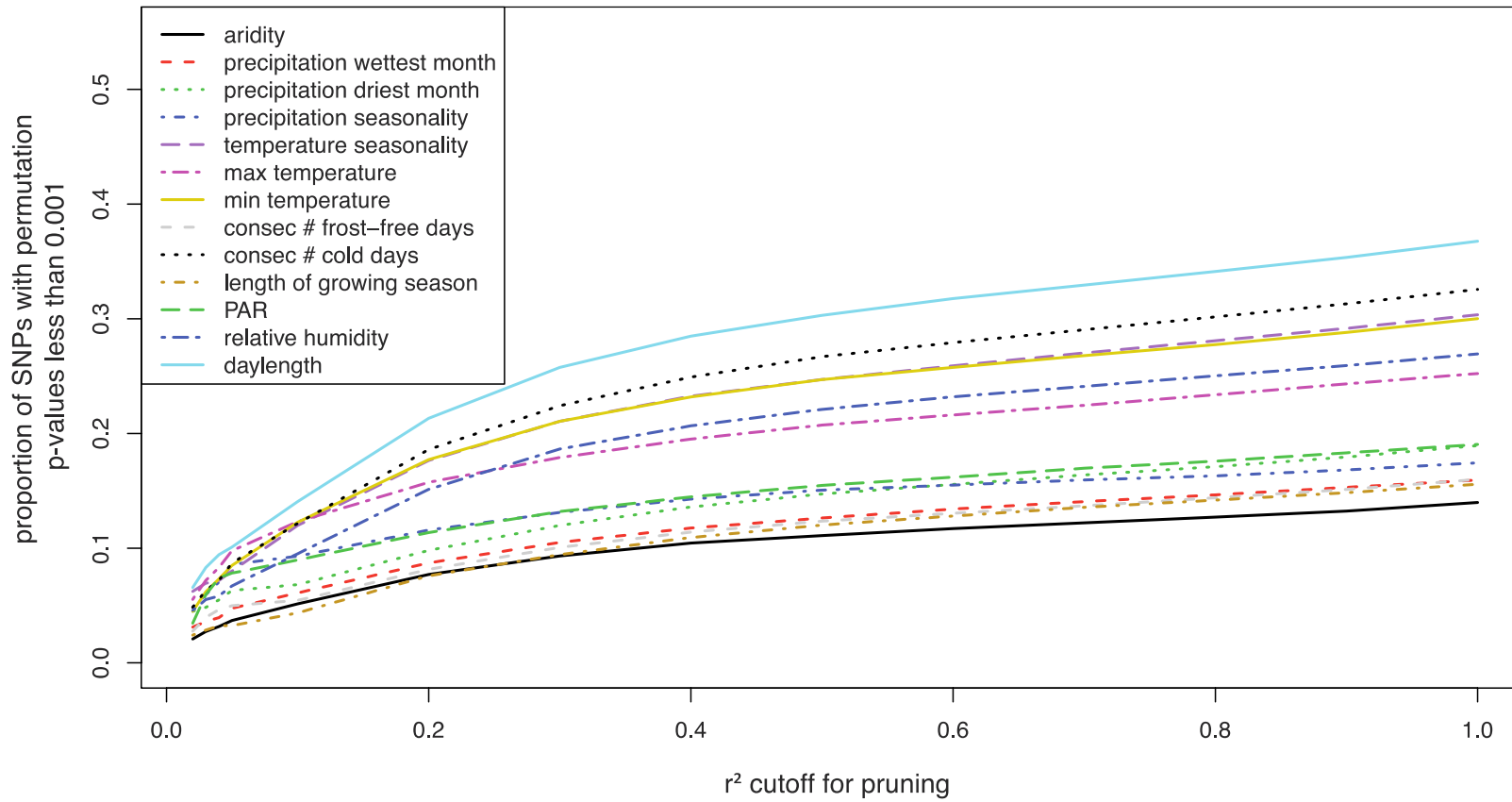
Distributions of the top 5 regions for relative humidity. For each SNP, the central sub-panel contains polygons showing the geographic extents of all 5 SNPs and sub-panels show the central feature and extent of each individual SNP.

Fig. S10



Correlation matrix of all climate variables

Fig. S11



Proportions of SNPs with permutation p-values less than 0.001 across SNP sets sampled to include varying levels of redundancy due to LD. An r^2 cutoff of 1 represents the case where all SNPs were included in the analysis and r^2 cutoffs near zero represent cases in which each SNP represents a nearly independent region of the genome.

Table S1.

Summary of 41 climate variables gathered for this analysis and sources of information.

| variable | source | grid resolution | url | reference |
|--|--|----------------------------|---|--|
| Length of the growing season (based on temperature and potential evaporation relative to precipitation by month) | FAO GeoNetwork | 0.5°x 0.5° grid (~55 km) | http://www.fao.org/geonetwork/srv/en/main.home | NA |
| Length of the growing season (based on temperature alone; by month) | | 5 arc-Minutes (~9 km) | | |
| Mean Temperature (winter) | WorldClim | 30 arc-seconds (~1 km) | http://www.worldclim.org/ | Hijmans, R.J., S.E. Cameron, J.L. Parra, P.G. Jones and A. Jarvis, 2005. Very high resolution interpolated climate surfaces for global land areas. |
| Mean Temperature (spring) | | | | International Journal of Climatology 25: 1965-1978. |
| Mean Temperature (summer) | | | | |
| Mean Temperature (fall) | | | | |
| Annual Mean Temperature | | | | |
| Mean Diurnal Range (Mean of monthly (max temp - min temp)) | | | | |
| Isothermality (P2/P7) (* 100) | | | | |
| Temperature Seasonality (standard deviation *100) | | | | |
| Max Temperature of Warmest Month | | | | |
| Min Temperature of Coldest Month | | | | |
| Temperature Annual Range (P5-P6) | | | | |
| Mean Temperature of Wettest Quarter | | | | |
| Mean Temperature of Driest Quarter | | | | |
| Mean Temperature of Warmest Quarter | | | | |
| Mean Temperature of Coldest Quarter | | | | |
| Annual Precipitation | | | | |
| Precipitation of Wettest Month | | | | |
| Precipitation of Driest Month | | | | |
| Precipitation Seasonality (Coefficient of Variation) | | | | |
| Precipitation of Wettest Quarter | | | | |
| Precipitation of Driest Quarter | | | | |
| Precipitation of Warmest Quarter | | | | |
| Precipitation of Coldest Quarter | | | | |
| Photosynthetically active radiation (fall) | NASA/GEWE X Surface Radiation Budget (SRB) | 1°x 1° grid (~111 km) | http://eosweb.larc.nasa.gov/PRODOCS/srb/table_srb.html | These data were obtained from the NASA Langley Research Center Atmospheric Science Data Center. |
| Photosynthetically active radiation (winter) | | | | |
| Photosynthetically active radiation (spring) | | | | |
| Photosynthetically active radiation (summer) | | | | |
| Number of consecutive cold days (below 4 degrees C) | NCDC | 0.37°x 0.37° grid (~40 km) | http://www.ncdc.noaa.gov/cgi-bin/res40.pl?page=gsod.html | The NCDC Climate Services Branch (CSB) |
| Number of consecutive frost-free days (above 0 degrees C) | | | | |
| Relative humidity (winter) | NCAR/NCEP | 5 arc-Minutes (~9 km) | http://iridl.ldeo.columbia.edu/SOURCES/.NOAA/.NCEP-.NCAR/.CDAS-1/.MONTHLY/.Intrinsic/.Pressure_Level/.rhum/ | Kalnay, E., M. Kanamitsu, R. Kistler, et all. The NCEP/NCAR 40-Year Reanalysis Project. Bulletin of the American Meteorological Society, March, 1996 |
| Relative humidity (summer) | | | | |
| Relative humidity (spring) | | | | |
| Relative humidity (fall) | | | | |
| Daylength (winter) | | NA | | Meeus, Jean. (1991) Astronomical algorithms. |
| Daylength (spring) | | | | Richmond, Va.: Willmann-Bell. |
| Daylength (summer) | | | | ISBN 0943396352 |
| Daylength (fall) | | | | |

Table S2.

Enrichment of biological processes in the 1% tail (with $p \leq 0.01$) for any of the 13 climate variables.

| Climate | Biological Process | Enrichment | p-value |
|------------------|---|------------|---------|
| aridity | pyridine nucleotide biosynthetic process | 17.39 | 0.001 |
| aridity | pyridine nucleotide biosynthetic process | 17.39 | 0.00097 |
| aridity | root hair initiation | 15.38 | 0.008 |
| aridity | base-excision repair | 13.59 | 0.00014 |
| aridity | two-component signal transduction system (phosphorelay) | 12.79 | 0.00013 |
| aridity | NAD(P)H dehydrogenase complex (plastoquinone) | 12.50 | 0.003 |
| aridity | glutamate decarboxylation to succinate | 11.76 | 0.006 |
| aridity | DNA replication initiation | 11.40 | 0.0006 |
| aridity | DNA unwinding during replication | 11.11 | 0.001 |
| aridity | starch metabolic process | 11.11 | 0.001 |
| aridity | DNA unwinding during replication | 11.11 | 0.00097 |
| aridity | starch metabolic process | 11.11 | 0.00106 |
| aridity | seed dormancy | 10.52 | 0.001 |
| aridity | N-glycan processing | 10.00 | 0.008 |
| aridity | protein import into chloroplast stroma | 9.75 | 0.007 |
| aridity | salicylic acid mediated signaling pathway | 9.09 | 0.002 |
| aridity | sugar mediated signaling pathway | 8.97 | 0.00036 |
| aridity | asparagine biosynthetic process | 8.33 | 0.008 |
| aridity | defense response, incompatible interaction | 7.69 | 0.007 |
| aridity | floral organ abscission | 6.97 | 0.006 |
| aridity | DNA topological change | 6.84 | 0.005 |
| aridity | sucrose biosynthetic process | 5.67 | 0.007 |
| aridity | response to virus | 5.52 | 0.004 |
| aridity | photosynthesis | 5.50 | 0.00106 |
| aridity | microtubule-based movement | 5.31 | 0.002 |
| aridity | microtubule-based movement | 5.31 | 0.00026 |
| aridity | positive regulation of flower development | 4.63 | 0.005 |
| aridity | glycolysis | 4.11 | 0.003 |
| aridity | regulation of cell cycle | 3.87 | 0.003 |
| aridity | vegetative to reproductive phase transition of meristem | 3.84 | 0.008 |
| aridity | response to stress | 3.07 | 0.005 |
| aridity | DNA repair | 2.82 | 0.004 |
| aridity | regulation of transcription | 1.63 | 0.008 |
| consec cold days | cytidine deamination | 26.66 | 0.003 |
| consec cold days | cytidine metabolic process | 26.66 | 0.005 |
| consec cold days | protein ubiquitination during ubiquitin-dependent protein catabolic process | 24.99 | 0.005 |
| consec cold days | regulation of actin filament polymerization | 19.99 | 0.005 |
| consec cold days | methylation-dependent chromatin silencing | 16.66 | 0.005 |
| consec cold days | Golgi vesicle transport | 15.68 | 0.005 |
| consec cold days | cellular aromatic compound metabolic process | 15.38 | 0.005 |
| consec cold days | plant-type cell wall organization | 14.75 | 0.001 |
| consec cold days | epidermal cell fate specification | 14.28 | 0.004 |
| consec cold days | mitochondrial electron transport, succinate to ubiquinone | 13.79 | 0.005 |
| consec cold days | protein import into nucleus | 13.33 | 0.001 |
| consec cold days | protein import into nucleus | 13.33 | 0.00014 |
| consec cold days | peptidyl-cysteine S-nitrosylation | 12.76 | 0.002 |
| consec cold days | post-translational protein modification | 12.50 | 0.001 |
| consec cold days | post-translational protein modification | 12.50 | 0.00056 |
| consec cold days | cell wall biogenesis | 12.30 | 0.004 |
| consec cold days | transcription initiation from RNA polymerase II promoter | 11.47 | 0.004 |
| consec cold days | regulation of protein metabolic process | 10.97 | 0.001 |
| consec cold days | cysteine biosynthetic process | 9.23 | 0.007 |
| consec cold days | D-ribose metabolic process | 8.82 | 0.003 |
| consec cold days | trichome differentiation | 8.33 | 0.006 |
| consec cold days | hyperosmotic response | 7.35 | 0.007 |

| | | | |
|------------------------|---|-------|---------|
| consec cold days | copper ion transport | 7.02 | 0.008 |
| consec cold days | aging | 6.28 | 0.001 |
| consec cold days | mRNA processing | 6.18 | 0.009 |
| consec cold days | multidrug transport | 4.94 | 0.001 |
| consec cold days | multidrug transport | 4.94 | 0.0009 |
| consec cold days | carbohydrate metabolic process | 1.91 | 0.009 |
| consec frost-free days | maintenance of root meristem identity | 25.71 | 0.00047 |
| consec frost-free days | indoleacetic acid biosynthetic process | 23.68 | 0.001 |
| consec frost-free days | threonine biosynthetic process | 18.74 | 0.001 |
| consec frost-free days | gynoecium development | 18.36 | 0.001 |
| consec frost-free days | cellular response to water deprivation | 18.18 | 0.002 |
| consec frost-free days | mitochondrial electron transport, NADH to ubiquinone | 17.85 | 0.002 |
| consec frost-free days | NAD(P)H dehydrogenase complex (plastoquinone) | 16.66 | 0.001 |
| consec frost-free days | epidermal cell differentiation | 16.39 | 0.002 |
| consec frost-free days | cotyledon vascular tissue pattern formation | 15.51 | 0.00083 |
| consec frost-free days | proteasomal ubiquitin-dependent protein catabolic process | 14.28 | 0.003 |
| consec frost-free days | positive gravitropism | 13.09 | 0.00031 |
| consec frost-free days | root epidermal cell differentiation | 12.50 | 0.003 |
| consec frost-free days | epidermal cell fate specification | 11.90 | 0.005 |
| consec frost-free days | regulation of chlorophyll biosynthetic process | 11.62 | 0.002 |
| consec frost-free days | two-component signal transduction system (phosphorelay) | 11.62 | 0.00038 |
| consec frost-free days | starch biosynthetic process | 8.74 | 0.003 |
| consec frost-free days | cotyledon development | 8.62 | 0.001 |
| consec frost-free days | cotyledon development | 8.62 | 0.00103 |
| consec frost-free days | tubulin complex assembly | 8.57 | 0.007 |
| consec frost-free days | cell morphogenesis | 7.69 | 0.009 |
| consec frost-free days | phloem or xylem histogenesis | 7.44 | 0.002 |
| consec frost-free days | mRNA processing | 7.30 | 0.001 |
| consec frost-free days | salicylic acid mediated signaling pathway | 7.27 | 0.003 |
| consec frost-free days | trichome differentiation | 7.14 | 0.009 |
| consec frost-free days | nucleotide-excision repair | 6.97 | 0.007 |
| consec frost-free days | protein targeting to vacuole | 6.89 | 0.004 |
| consec frost-free days | cellular amino acid biosynthetic process | 6.66 | 0.009 |
| consec frost-free days | microtubule-based movement | 6.58 | 0.001 |
| consec frost-free days | microtubule-based movement | 6.58 | 0.00005 |
| consec frost-free days | photorespiration | 6.29 | 0.002 |
| consec frost-free days | double fertilization forming a zygote and endosperm | 5.64 | 0.006 |
| consec frost-free days | cytokinin mediated signaling pathway | 4.22 | 0.002 |
| consec frost-free days | flower development | 3.65 | 0.002 |
| consec frost-free days | DNA repair | 3.20 | 0.005 |
| daylength | regulation of signal transduction | 26.66 | 0.00024 |
| daylength | SCF-dependent proteasomal ubiquitin-dependent protein catabolic process | 22.22 | 0.002 |
| daylength | cytidine deamination | 19.99 | 0.004 |
| daylength | cytidine metabolic process | 19.99 | 0.004 |
| daylength | methylation-dependent chromatin silencing | 16.66 | 0.002 |
| daylength | jasmonic acid and ethylene-dependent systemic resistance | 16.00 | 0.004 |
| daylength | epidermal cell fate specification | 14.28 | 0.003 |
| daylength | amylopectin biosynthetic process | 12.50 | 0.002 |
| daylength | histone modification | 10.00 | 0.006 |
| daylength | trichome differentiation | 9.52 | 0.001 |
| daylength | sodium ion transport | 8.94 | 0.003 |
| daylength | sodium ion transport | 8.94 | 0.00079 |
| daylength | post-translational protein modification | 8.33 | 0.003 |
| daylength | maintenance of floral meristem identity | 7.69 | 0.008 |
| daylength | cysteine biosynthetic process | 7.69 | 0.005 |
| daylength | hyperosmotic response | 7.35 | 0.007 |
| daylength | regulation of protein metabolic process | 7.31 | 0.006 |
| daylength | methionine biosynthetic process | 6.78 | 0.007 |
| daylength | response to virus | 5.52 | 0.007 |
| daylength | photomorphogenesis | 4.08 | 0.002 |
| daylength | response to salicylic acid stimulus | 3.13 | 0.003 |
| daylength | carbohydrate metabolic process | 2.25 | 0.00293 |
| growing season length | mitochondrial electron transport, NADH to ubiquinone | 24.99 | 0.001 |

| | | | |
|-----------------------|---|-------|---------|
| growing season length | mitochondrial electron transport, NADH to ubiquinone | 24.99 | 0.0005 |
| growing season length | asparagine biosynthetic process | 16.66 | 0.003 |
| growing season length | seed oilbody biogenesis | 15.38 | 0.002 |
| growing season length | tubulin complex assembly | 14.28 | 0.002 |
| growing season length | protein sumoylation | 13.63 | 0.002 |
| growing season length | base-excision repair | 13.59 | 0.00008 |
| growing season length | epidermal cell differentiation | 13.11 | 0.0003 |
| growing season length | photoinhibition | 11.76 | 0.002 |
| growing season length | peptidyl-cysteine S-nitrosylation | 10.64 | 0.001 |
| growing season length | mitochondrial electron transport, succinate to ubiquinone | 10.34 | 0.006 |
| growing season length | nucleotide-sugar transport | 10.00 | 0.001 |
| growing season length | N-glycan processing | 10.00 | 0.007 |
| growing season length | epidermal cell fate specification | 9.52 | 0.008 |
| growing season length | PSII associated light-harvesting complex II catabolic process | 8.82 | 0.004 |
| growing season length | vernization response | 8.41 | 0.001 |
| growing season length | regulation of meristem growth | 6.82 | 0.008 |
| growing season length | chloroplast RNA processing | 6.25 | 0.009 |
| growing season length | response to virus | 6.21 | 0.005 |
| growing season length | folic acid and derivative biosynthetic process | 5.88 | 0.009 |
| growing season length | negative regulation of flower development | 4.76 | 0.001 |
| growing season length | amino acid transport | 4.04 | 0.003 |
| growing season length | DNA repair | 3.08 | 0.001 |
| growing season length | embryonic development ending in seed dormancy | 2.25 | 0.00022 |
| growing season length | regulation of transcription | 1.66 | 0.003 |
| max T (warmest month) | L-phenylalanine biosynthetic process | 18.60 | 0.00039 |
| max T (warmest month) | mitochondrial electron transport, NADH to ubiquinone | 17.85 | 0.008 |
| max T (warmest month) | defense response signaling pathway, resistance gene-independent | 14.28 | 0.00086 |
| max T (warmest month) | translational termination | 12.30 | 0.001 |
| max T (warmest month) | regulation of nitrogen utilization | 12.24 | 0.001 |
| max T (warmest month) | galactolipid biosynthetic process | 12.12 | 0.005 |
| max T (warmest month) | mRNA cleavage involved in gene silencing by miRNA | 11.53 | 0.009 |
| max T (warmest month) | unsaturated fatty acid biosynthetic process | 11.11 | 0.007 |
| max T (warmest month) | plastid organization | 8.75 | 0.005 |
| max T (warmest month) | tRNA processing | 8.57 | 0.001 |
| max T (warmest month) | tRNA processing | 8.57 | 0.00005 |
| max T (warmest month) | polysaccharide biosynthetic process | 7.84 | 0.003 |
| max T (warmest month) | histone deacetylation | 7.84 | 0.004 |
| max T (warmest month) | tricarboxylic acid cycle | 7.69 | 0.003 |
| max T (warmest month) | nuclear mRNA splicing, via spliceosome | 7.36 | 0.001 |
| max T (warmest month) | nuclear mRNA splicing, via spliceosome | 7.36 | 0.00049 |
| max T (warmest month) | red, far-red light phototransduction | 7.14 | 0.007 |
| max T (warmest month) | reciprocal meiotic recombination | 6.25 | 0.006 |
| max T (warmest month) | response to cyclopentenone | 5.80 | 0.003 |
| max T (warmest month) | photoperiodism, flowering | 4.54 | 0.008 |
| max T (warmest month) | DNA mediated transformation | 4.52 | 0.006 |
| max T (warmest month) | trichome morphogenesis | 4.23 | 0.007 |
| max T (warmest month) | cell wall modification | 3.81 | 0.003 |
| max T (warmest month) | oxidation reduction | 2.80 | 0.005 |
| max T (warmest month) | response to cadmium ion | 2.69 | 0.00031 |
| max T (warmest month) | response to cold | 2.52 | 0.003 |
| min T (coldest month) | regulation of signal transduction | 26.66 | 0.00032 |
| min T (coldest month) | cytidine deamination | 19.99 | 0.004 |
| min T (coldest month) | regulation of actin filament polymerization | 19.99 | 0.005 |
| min T (coldest month) | cytidine metabolic process | 19.99 | 0.008 |
| min T (coldest month) | threonine biosynthetic process | 18.74 | 0.003 |
| min T (coldest month) | SCF-dependent proteasomal ubiquitin-dependent protein catabolic process | 16.66 | 0.004 |
| min T (coldest month) | epidermal cell fate specification | 14.28 | 0.006 |
| min T (coldest month) | glycerol-3-phosphate metabolic process | 12.50 | 0.005 |
| min T (coldest month) | jasmonic acid and ethylene-dependent systemic resistance | 12.00 | 0.007 |
| min T (coldest month) | amylopectin biosynthetic process | 10.00 | 0.008 |
| min T (coldest month) | post-translational protein modification | 9.72 | 0.002 |
| min T (coldest month) | trichome differentiation | 9.52 | 0.001 |
| min T (coldest month) | cysteine biosynthetic process | 9.23 | 0.003 |

| | | | |
|-----------------------|---|-------|---------|
| min T (coldest month) | copper ion transport | 8.77 | 0.006 |
| min T (coldest month) | regulation of protein metabolic process | 8.53 | 0.009 |
| min T (coldest month) | protein import into nucleus | 8.33 | 0.006 |
| min T (coldest month) | hyperosmotic response | 7.35 | 0.005 |
| min T (coldest month) | D-ribose metabolic process | 7.35 | 0.008 |
| min T (coldest month) | protein targeting to vacuole | 6.89 | 0.004 |
| min T (coldest month) | response to gibberellin stimulus | 5.36 | 0.001 |
| min T (coldest month) | response to gibberellin stimulus | 5.36 | 0.0004 |
| min T (coldest month) | pollen germination | 4.40 | 0.005 |
| min T (coldest month) | response to salicylic acid stimulus | 3.97 | 0.002 |
| min T (coldest month) | defense response to fungus | 3.47 | 0.009 |
| min T (coldest month) | response to jasmonic acid stimulus | 2.97 | 0.004 |
| min T (coldest month) | response to cadmium ion | 2.63 | 0.00047 |
| min T (coldest month) | response to salt stress | 2.39 | 0.002 |
| min T (coldest month) | carbohydrate metabolic process | 1.96 | 0.005 |
| PAR | maintenance of root meristem identity | 31.42 | 0.00001 |
| PAR | indoleacetic acid biosynthetic process | 28.94 | 0.00001 |
| PAR | cellular response to water deprivation | 27.26 | 0.00006 |
| PAR | regulation of defense response | 24.24 | 0.00028 |
| PAR | gynoecium development | 22.44 | 0.00002 |
| PAR | red light signaling pathway | 21.62 | 0.00014 |
| PAR | stomatal complex development | 21.62 | 0.00011 |
| PAR | cotyledon vascular tissue pattern formation | 18.96 | 0.00005 |
| PAR | mitochondrial electron transport, NADH to ubiquinone | 17.85 | 0.001 |
| PAR | NAD(P)H dehydrogenase complex (plastoquinone) | 16.66 | 0.001 |
| PAR | jasmonic acid and ethylene-dependent systemic resistance | 16.00 | 0.002 |
| PAR | positive gravitropism | 15.47 | 0.00001 |
| PAR | root hair initiation | 15.38 | 0.009 |
| PAR | methionine metabolic process | 12.50 | 0.007 |
| PAR | induced systemic resistance, jasmonic acid mediated signaling pathway | 11.53 | 0.008 |
| PAR | tyrosine biosynthetic process | 11.11 | 0.002 |
| PAR | protein deubiquitination | 11.11 | 0.009 |
| PAR | cotyledon development | 10.34 | 0.001 |
| PAR | cotyledon development | 10.34 | 0.00021 |
| PAR | leucine biosynthetic process | 9.61 | 0.003 |
| PAR | proanthocyanidin biosynthetic process | 9.26 | 0.006 |
| PAR | phloem or xylem histogenesis | 9.09 | 0.00031 |
| PAR | base-excision repair | 8.74 | 0.004 |
| PAR | tubulin complex assembly | 8.57 | 0.009 |
| PAR | gravitropism | 8.33 | 0.001 |
| PAR | regulation of seed germination | 7.87 | 0.003 |
| PAR | starch biosynthetic process | 7.76 | 0.005 |
| PAR | jasmonic acid mediated signaling pathway | 7.57 | 0.001 |
| PAR | phototropism | 7.50 | 0.005 |
| PAR | thylakoid membrane organization | 6.06 | 0.005 |
| PAR | lactose catabolic process, using glucoside 3-dehydrogenase | 6.00 | 0.007 |
| PAR | systemic acquired resistance | 5.62 | 0.004 |
| PAR | photosynthesis | 4.59 | 0.001 |
| PAR | photosynthesis | 4.59 | 0.007 |
| PAR | regulation of stomatal movement | 4.52 | 0.006 |
| PAR | positive regulation of transcription | 4.37 | 0.004 |
| PAR | vegetative to reproductive phase transition of meristem | 4.27 | 0.008 |
| PAR | seed development | 3.74 | 0.009 |
| PAR | flower development | 3.16 | 0.003 |
| PAR | response to cold | 2.98 | 0.0069 |
| PAR | regulation of transcription, DNA-dependent | 1.89 | 0.001 |
| precip (driest month) | maintenance of root meristem identity | 22.85 | 0.00036 |
| precip (driest month) | indoleacetic acid biosynthetic process | 21.05 | 0.00013 |
| precip (driest month) | mitochondrial electron transport, succinate to ubiquinone | 20.68 | 0.001 |
| precip (driest month) | cotyledon vascular tissue pattern formation | 13.79 | 0.001 |
| precip (driest month) | glucuronoxylan biosynthetic process | 13.04 | 0.005 |
| precip (driest month) | epidermal cell fate specification | 11.90 | 0.002 |
| precip (driest month) | peptidyl-cysteine S-nitrosylation | 10.64 | 0.001 |

| | | | |
|------------------------|---|-------|---------|
| precip (driest month) | positive gravitropism | 9.52 | 0.002 |
| precip (driest month) | L-phenylalanine biosynthetic process | 9.30 | 0.002 |
| precip (driest month) | specification of floral organ identity | 8.00 | 0.009 |
| precip (driest month) | cell adhesion | 7.84 | 0.006 |
| precip (driest month) | cotyledon development | 7.76 | 0.001 |
| precip (driest month) | DNA mediated transformation | 5.08 | 0.001 |
| precip (driest month) | DNA replication | 4.01 | 0.002 |
| precip (driest month) | flower development | 3.41 | 0.007 |
| precip (driest month) | intracellular protein transport | 2.33 | 0.006 |
| precip (wettest month) | pyridine nucleotide biosynthetic process | 17.39 | 0.00068 |
| precip (wettest month) | mitochondrial electron transport, NADH to ubiquinone | 14.28 | 0.005 |
| precip (wettest month) | base-excision repair | 13.59 | 0.00009 |
| precip (wettest month) | hyperosmotic response | 11.76 | 0.002 |
| precip (wettest month) | glutamate decarboxylation to succinate | 11.76 | 0.005 |
| precip (wettest month) | root hair cell tip growth | 11.68 | 0.001 |
| precip (wettest month) | signal peptide processing | 11.43 | 0.003 |
| precip (wettest month) | stomatal complex morphogenesis | 11.11 | 0.00074 |
| precip (wettest month) | nicotianamine biosynthetic process | 11.11 | 0.006 |
| precip (wettest month) | seed dormancy | 10.52 | 0.002 |
| precip (wettest month) | amylopectin biosynthetic process | 10.00 | 0.004 |
| precip (wettest month) | N-glycan processing | 10.00 | 0.006 |
| precip (wettest month) | starch metabolic process | 9.72 | 0.001 |
| precip (wettest month) | starch metabolic process | 9.72 | 0.002 |
| precip (wettest month) | PSII associated light-harvesting complex II catabolic process | 8.82 | 0.007 |
| precip (wettest month) | photoinhibition | 8.82 | 0.004 |
| precip (wettest month) | post-embryonic root development | 8.33 | 0.008 |
| precip (wettest month) | salicylic acid mediated signaling pathway | 7.27 | 0.005 |
| precip (wettest month) | protein catabolic process | 6.42 | 0.00029 |
| precip (wettest month) | defense response, incompatible interaction | 6.15 | 0.007 |
| precip (wettest month) | response to abiotic stimulus | 6.00 | 0.008 |
| precip (wettest month) | cell division | 5.75 | 0.001 |
| precip (wettest month) | cell division | 5.75 | 0.0003 |
| precip (wettest month) | organ morphogenesis | 5.26 | 0.005 |
| precip (wettest month) | thylakoid membrane organization | 4.54 | 0.006 |
| precip (wettest month) | vegetative to reproductive phase transition of meristem | 4.27 | 0.003 |
| precip (wettest month) | cell wall modification | 3.17 | 0.006 |
| precip (wettest month) | translational initiation | 3.13 | 0.007 |
| precip (wettest month) | vesicle-mediated transport | 2.56 | 0.004 |
| precip seasonality | maintenance of root meristem identity | 22.85 | 0.00115 |
| precip seasonality | mitochondrial electron transport, NADH to ubiquinone | 17.85 | 0.006 |
| precip seasonality | gynoecium development | 16.32 | 0.001 |
| precip seasonality | protein import into nucleus | 15.00 | 0.00021 |
| precip seasonality | response to symbiotic fungus | 14.28 | 0.003 |
| precip seasonality | cotyledon vascular tissue pattern formation | 13.79 | 0.002 |
| precip seasonality | secondary shoot formation | 12.50 | 0.006 |
| precip seasonality | lipid storage | 12.19 | 0.001 |
| precip seasonality | coenzyme A biosynthetic process | 10.81 | 0.006 |
| precip seasonality | positive gravitropism | 9.52 | 0.004 |
| precip seasonality | very-long-chain fatty acid metabolic process | 7.84 | 0.008 |
| precip seasonality | cotyledon development | 7.76 | 0.002 |
| precip seasonality | cuticle development | 7.54 | 0.005 |
| precip seasonality | cell death | 7.00 | 0.001 |
| precip seasonality | phloem or xylem histogenesis | 6.61 | 0.005 |
| precip seasonality | toxin catabolic process | 6.01 | 0.008 |
| precip seasonality | mismatch repair | 5.73 | 0.006 |
| precip seasonality | negative regulation of flower development | 5.08 | 0.004 |
| precip seasonality | response to ethylene stimulus | 3.54 | 0.004 |
| precip seasonality | flower development | 3.41 | 0.009 |
| relative humidity | regulation of signal transduction | 29.99 | 0.001 |
| relative humidity | folic acid and derivative metabolic process | 23.07 | 0.003 |
| relative humidity | glucuronoxylan biosynthetic process | 17.39 | 0.004 |
| relative humidity | signal peptide processing | 17.14 | 0.001 |
| relative humidity | asparagine biosynthetic process | 16.66 | 0.007 |
| relative humidity | mitochondrial electron transport, NADH to ubiquinone | 14.28 | 0.009 |

| | | | |
|-------------------|---|-------|---------|
| relative humidity | synapsis | 12.30 | 0.0005 |
| relative humidity | cellular component organization | 11.43 | 0.005 |
| relative humidity | meristem development | 10.97 | 0.003 |
| relative humidity | peptidyl-cysteine S-nitrosylation | 10.64 | 0.002 |
| relative humidity | sister chromatid cohesion | 10.57 | 0.002 |
| relative humidity | electron transport chain | 10.00 | 0.009 |
| relative humidity | epidermal cell fate specification | 9.52 | 0.008 |
| relative humidity | reciprocal meiotic recombination | 8.93 | 0.001 |
| relative humidity | oxygen and reactive oxygen species metabolic process | 8.66 | 0.002 |
| relative humidity | protein import into nucleus | 8.33 | 0.001 |
| relative humidity | specification of floral organ identity | 8.00 | 0.009 |
| relative humidity | microsporogenesis | 6.33 | 0.004 |
| relative humidity | actin cytoskeleton organization | 5.88 | 0.006 |
| relative humidity | intracellular protein transport | 2.67 | 0.004 |
| relative humidity | response to salt stress | 2.27 | 0.004 |
| temp seasonality | regulation of signal transduction | 26.66 | 0.00052 |
| temp seasonality | cytidine deamination | 19.99 | 0.009 |
| temp seasonality | cytidine metabolic process | 19.99 | 0.007 |
| temp seasonality | electron transport chain | 15.00 | 0.003 |
| temp seasonality | base-excision repair | 12.62 | 0.00042 |
| temp seasonality | trichome differentiation | 9.52 | 0.006 |
| temp seasonality | negative regulation of seed germination | 9.30 | 0.004 |
| temp seasonality | auxin biosynthetic process | 9.26 | 0.007 |
| temp seasonality | cysteine biosynthetic process | 9.23 | 0.009 |
| temp seasonality | protein targeting to vacuole | 8.62 | 0.001 |
| temp seasonality | two-component signal transduction system (phosphorelay) | 8.14 | 0.003 |
| temp seasonality | mRNA processing | 7.86 | 0.001 |
| temp seasonality | salicylic acid mediated signaling pathway | 7.27 | 0.008 |
| temp seasonality | gravitropism | 6.66 | 0.009 |
| temp seasonality | response to gibberellin stimulus | 5.06 | 0.001 |
| temp seasonality | pollen tube growth | 4.69 | 0.002 |
| temp seasonality | pollen germination | 4.40 | 0.008 |
| temp seasonality | response to salicylic acid stimulus | 3.55 | 0.004 |
| temp seasonality | microtubule-based movement | 3.40 | 0.008 |
| temp seasonality | DNA repair | 3.20 | 0.004 |
| temp seasonality | response to auxin stimulus | 2.85 | 0.003 |
| temp seasonality | response to salt stress | 2.08 | 0.004 |
| temp seasonality | protein amino acid phosphorylation | 1.69 | 0.008 |

References and Notes

1. W. E. Bradshaw, C. M. Holzapfel, Genetic shift in photoperiodic response correlated with global warming. *Proc. Natl. Acad. Sci. U.S.A.* **98**, 14509 (2001).
2. S. J. Franks, S. Sim, A. E. Weis, Rapid evolution of flowering time by an annual plant in response to a climate fluctuation. *Proc. Natl. Acad. Sci. U.S.A.* **104**, 1278 (2007).
3. D. B. Lobell, W. Schlenker, J. Costa-Roberts, Climate trends and global crop production since 1980. *Science* **333**, 616 (2011).
4. M. Lynch, R. Lande, in *Biotic Interactions and Global Change*, P. M. Kareiva, J. G. Kingsolver, R. B. Huey, Eds. (Sinauer Associates, Sunderland, MA, 1993), pp. 234–250.
5. P. A. Umina, A. R. Weeks, M. R. Kearney, S. W. McKechnie, A. A. Hoffmann, A rapid shift in a classic clinal pattern in *Drosophila* reflecting climate change. *Science* **308**, 691 (2005).
6. A. A. Hoffmann, C. M. Sgrò, Climate change and evolutionary adaptation. *Nature* **470**, 479 (2011).
7. S. Atwell *et al.*, Genome-wide association study of 107 phenotypes in *Arabidopsis thaliana* inbred lines. *Nature* **465**, 627 (2010).
8. J. Bergelson, F. Roux, Towards identifying genes underlying ecologically relevant traits in *Arabidopsis thaliana*. *Nat. Rev. Genet.* **11**, 867 (2010).
9. B. Brachi *et al.*, Linkage and association mapping of *Arabidopsis thaliana* flowering time in nature. *PLoS Genet.* **6**, e1000940 (2010).
10. C. Weinig *et al.*, Novel loci control variation in reproductive timing in *Arabidopsis thaliana* in natural environments. *Genetics* **162**, 1875 (2002).
11. D. H. Kim, M. R. Doyle, S. Sung, R. M. Amasino, Vernalization: Winter and the timing of flowering in plants. *Annu. Rev. Cell Dev. Biol.* **25**, 277 (2009).
12. B. Rathcke, E. P. Lacey, Phenological patterns of terrestrial plants. *Annu. Rev. Ecol. Syst.* **16**, 179 (1985).
13. See supporting material in *Science* Online.
14. A. M. Hancock *et al.*, Adaptations to climate-mediated selective pressures in humans. *PLoS Genet.* **7**, e1001375 (2011).
15. B. Charlesworth, M. T. Morgan, D. Charlesworth, The effect of deleterious mutations on neutral molecular variation. *Genetics* **134**, 1289 (1993).
16. J. H. Gillespie, Genetic drift in an infinite population. The pseudohitchhiking model. *Genetics* **155**, 909 (2000).
17. H.-u, -R. Athar, M. Ashraf, in *Handbook of Photosynthesis*, M. Pessarakli, Ed. (CRC Press, Boca Raton, FL, 2005), p. 928.
18. H. A. Orr, Adaptation and the cost of complexity. *Evolution* **54**, 13 (2000).

19. Z. Wang, B. Y. Liao, J. Zhang, Genomic patterns of pleiotropy and the evolution of complexity. *Proc. Natl. Acad. Sci. U.S.A.* **107**, 18034 (2010).
20. G. P. Wagner, J. Zhang, The pleiotropic structure of the genotype-phenotype map: The evolvability of complex organisms. *Nat. Rev. Genet.* **12**, 204 (2011).
21. F. Roux, J. Gasquez, X. Reboud, The dominance of the herbicide resistance cost in several *Arabidopsis thaliana* mutant lines. *Genetics* **166**, 449 (2004).
22. C. Toomajian *et al.*, A nonparametric test reveals selection for rapid flowering in the *Arabidopsis* genome. *PLoS Biol.* **4**, e137 (2006).
23. A. E. Anastasio *et al.*, Source verification of mis-identified *Arabidopsis thaliana* accessions. *Plant J.* **67**, 554 (2011).
24. R. J. Hijmans, S. E. Cameron, J. L. Parra, P. G. Jones, A. Jarvis, Very high resolution interpolated climate surfaces for global land areas. *Int. J. Climatol.* **25**, 1965 (2005).
25. R. Kistler *et al.*, The NCEP-NCAR 50-year reanalysis: Monthly means CD-ROM and documentation. *Bull. Am. Meteorol. Soc.* **82**, 247 (2001).
26. N. Mantel, The detection of disease clustering and a generalized regression approach. *Cancer Res.* **27**, 209 (1967).
27. P. E. Smouse, J. C. Long, R. R. Sokal, Multiple regression and correlation extensions of the Mantel test of matrix correspondence. *Syst. Biol.* **35**, 627 (1986).
28. S. C. Goslee, D. L. Urban, The ecodist package for dissimilarity-based analysis of ecological data. *J. Stat. Softw.* **22**, 1 (2007).
29. R Development Core Team, *R: A Language and Environment for Statistical Computing* (R Foundation for Statistical Computing, Vienna, Austria, 2009).
30. G. Coop, D. Witonsky, A. Di Rienzo, J. K. Pritchard, Using environmental correlations to identify loci underlying local adaptation. *Genetics* **185**, 1411 (2010).
31. S. Purcell *et al.*, PLINK: A tool set for whole-genome association and population-based linkage analyses. *Am. J. Hum. Genet.* **81**, 559 (2007).
32. F. Roux, L. Gao, J. Bergelson, Impact of initial pathogen density on resistance and tolerance in a polymorphic disease resistance gene system in *Arabidopsis thaliana*. *Genetics* **185**, 283 (2010).
33. H. M. Kang *et al.*, Efficient control of population structure in model organism association mapping. *Genetics* **178**, 1709 (2008).
34. Gene Ontology Consortium, The Gene Ontology project in 2008. *Nucleic Acids Res.* **36** (Database issue), D440 (2008).
35. A. R. Walker *et al.*, The TRANSPARENT TESTA GLABRA1 locus, which regulates trichome differentiation and anthocyanin biosynthesis in *Arabidopsis*, encodes a WD40 repeat protein. *Plant Cell* **11**, 1337 (1999).